Submitted to the Journal of
the Electrochemical Society

LBL-2596
Preprint c.2

MASS TRANSFER OF MINOR COMPONENTS IN A PROPAGATING CRACK

William H. Smyrl and John Newman

RECEIVED
LAWRENCE
RADIATION LABORATORY

APR 5 1974

LIBRARY AND
DOCUMENTS SECTION

March 1974

Prepared for the U. S. Atomic Energy Commission
under Contract W-7405-ENG-48

TWO-WEEK LOAN COPY

This is a Library Circulating Copy which may be borrowed for two weeks. For a personal retention copy, call Tech. Info. Division, Ext. 5545

LAWRENCE BERKELEY LABORATORY
UNIVERSITY OF CALIFORNIA
BERKELEY

LBL-2596
c.2

25

DISCLAIMER

This document was prepared as an account of work sponsored by the United States Government. While this document is believed to contain correct information, neither the United States Government nor any agency thereof, nor the Regents of the University of California, nor any of their employees, makes any warranty, express or implied, or assumes any legal responsibility for the accuracy, completeness, or usefulness of any information, apparatus, product, or process disclosed, or represents that its use would not infringe privately owned rights. Reference herein to any specific commercial product, process, or service by its trade name, trademark, manufacturer, or otherwise, does not necessarily constitute or imply its endorsement, recommendation, or favoring by the United States Government or any agency thereof, or the Regents of the University of California. The views and opinions of authors expressed herein do not necessarily state or reflect those of the United States Government or any agency thereof or the Regents of the University of California.

Mass Transfer of Minor Components in a Propagating Crack*

William H. Smyrl
Sandia Laboratories
Albuquerque, New Mexico

and

John Newman
Inorganic Materials Research Division
Lawrence Berkeley Laboratory, and
Department of Chemical Engineering
University of California, Berkeley, Ca.

March 1974

ABSTRACT

The mass transfer of a dilute species in a liquid in a propagating crack is treated. The analysis includes the effect of convective flow of the liquid. The results of the calculations show that the crack tip is devoid of the minor species and that the mass flux of this component is also negligible in this region. Therefore, this could not be the critical species which causes cracking.

*This work was supported by the U.S. Atomic Energy Commission.

This was paper 244 presented at the Chicago, Illinois, Meeting of the Society, May 13-18, 1973.

Mass Transfer of Minor Components in a Propagating Crack

Introduction

The failure of structural materials such as metals and their alloys by stress corrosion cracking is a complex phenomena which involves the interplay of metallurgical, mechanical, and environmental influences. For an alloy of a particular metallurgical condition in a constant environment, the crack propagation may be investigated as a function of stress intensity*, a mechanical variable. It is generally found for titanium and aluminum alloys (1,2,3) that the rate of crack extension is dependent on the stress intensity at low stress levels but becomes independent of the stress intensity at higher levels. The process which limits the crack velocity at high stress intensities has been postulated to be a mass transfer limited process in the environment (4,5,6).

If the crack velocity is limited by the rate of mass transfer of a critical species to the crack tip, it would be expected that the velocity would decrease as the concentration of the species is decreased in the environment. In the limit of very small concentrations of this species, the crack velocity should approach that found in the pure environment. The present investigation was undertaken to quantify this relationship between the cracking rate and the mass transfer behavior of dilute species. The results should make it possible to evaluate the role of such components in a given stress corrosion cracking situation.

The specific system chosen for study was Titanium-8% Aluminum- 1% Molybdenum- 1% Vanadium in molten LiCl-KCl eutectic. This alloy has been shown to be susceptible to cracking in this environment (7), with crack rates up to a plateau rate of 1 cm/sec. The eutectic was obtained commercially in very pure form, with water as the major contaminant. The concentration of water was specified to be less than 0.1 ppm. Thus we are interested in the concentration and mass flux of this minor species (as a source of hydrogen) at the stress corrosion crack tip in the molten salt. The results should indicate whether a hydrogen model for crack extension could account for the high cracking velocities observed.

---

*The stress intensity is related to the stress, flaw size, and specimen geometry for materials which obey the laws of linear elastic fracture mechanics (1,2).

Model

The physical model to be treated here is sketched in Figure 1. The crack is wedge-shaped, with a geometrically-sharp tip, and extends through the thickness of the material. The coordinate system moves with the crack tip, so that the sides of the crack appear to move with the velocity V (1 cm/sec for LiCl-KCl) away from the tip. The flow pattern of the liquid has been determined from a treatment of the fluid mechanics of the system (8) and is shown also in this figure. The assumption will be adopted here that these velocity profiles are not changed by the mass transfer processes which we are considering. This is justified by the small concentration of the species of interest and may be checked by using the results which are obtained below. The inclusion of convective effects on mass transfer has not been considered previously for stress-corrosion calculations.

The steady-state velocity profiles in the liquid were found to be, for a small crack angle, $2\theta_w$,

$$v_r = -\frac{V}{2}\left\{1-3\frac{\theta^2}{\theta_w^2}\right\} \quad \text{(radial component)} \tag{1}$$

$$v_\theta = \frac{V\theta}{2}\left\{1-\frac{\theta^2}{\theta_w^2}\right\}. \quad \text{(angular component)} \tag{2}$$

These relationships are valid near the crack tip and out to distances from the crack tip of

$$r = O\left(47\frac{\nu}{\theta_w^2 V}\right).$$

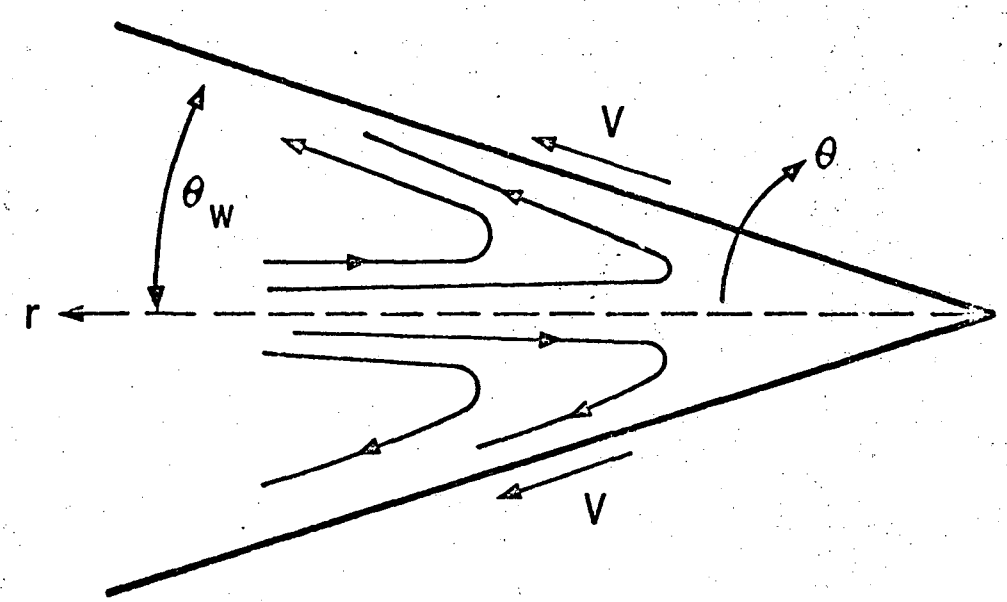

FIGURE 1. FLUID FLOW IN A PROPAGATING CRACK

With the physical properties of molten LiCl-KCl and a crack angle, $2\,\theta_w$, of 10^{-2} radians, this amounts to

$$r = O(10^{+3}\text{cm}).$$

At greater distances from the crack tip, inertial and pressure forces determine the fluid-flow characteristics, except near the crack walls where viscous forces are also important. We shall not be interested in such large distances from the crack tip except for completeness. Also, seepage of liquid in from the sides of the crack for plates of finite thickness becomes important at distances from the crack tip where the thickness is of the same order as $\theta_w r$.

The equation of convective diffusion for this system is, at steady-state,

$$v_r \frac{\partial c}{\partial r} + \frac{v_\theta}{r}\frac{\partial c}{\partial \theta} = D\left(\frac{\partial^2 c}{\partial r^2} + \frac{1}{r}\frac{\partial c}{\partial r} + \frac{1}{r^2}\frac{\partial^2 c}{\partial \theta^2}\right) \tag{3}$$

where c = concentration

D = diffusion coefficient

and v_r, v_θ are given by (1) and (2).

The boundary conditions are

$$c = 0 \text{ at crack wall} \tag{4}$$

$$c \to c_\infty \text{ at } \theta = 0,\ r \to \infty. \tag{5}$$

An auxiliary condition is

$$\frac{\partial c}{\partial \theta} = 0 \text{ at } \theta = 0, \tag{6}$$

since by symmetry there is no transfer of material across the crack center line. Equation (3) is valid for uncharged species, or for charged species where migration effects are not important. Migration makes no substantial contribution to equation (3) for our case because the concentration of any minor species is small as compared to that of K^+, Li^+, and Cl^-. The

boundary conditions are appropriate when the species, H_2O, is being consumed (reduced) at limiting current. Since most of the stress-corrosion tests have been carried out under potentiostatic conditions, almost to the lithium deposition potential, this is justified.

As additional justification for the treatment to follow, one may note that this is a simple system mathematically, and yet the results should be realistic. The results should also provide insight into the kind of improvements that could be made for future investigations.

Mathematical Treatment

For cracks of small angle, the θ-dimension can be scaled accordingly, and the distance from the crack tip can be made dimensionless in such a way that different regions of mass transfer are revealed.

Introduction of the new variables

$$\theta^* = (\theta/\theta_w)$$

$$r^* = \frac{rV}{D} (\theta_w)^2$$

into equation (3) yields

$$- \frac{1}{2}(1-3\theta^{*2}) \frac{\partial c}{\partial r^*} + \frac{1}{2}\theta^* \frac{(1-\theta^{*2})}{r^*} \frac{\partial c}{\partial \theta^*} =$$

$$\frac{1}{r^{*2}} \frac{\partial^2 c}{\partial \theta^{*2}} + \theta_w^{\ 2} \left(\frac{\partial^2 c}{\partial r^{*2}} + \frac{1}{r^*} \frac{\partial c}{\partial r^*} \right) . \qquad (7)$$

The last two terms, which contain the contribution of radial diffusion, may be discarded except for very small values of r^*. Since appreciable mass transfer occurs only at larger values of r^*, we neglect these radial-diffusion terms in the remainder of this work.

The radial convection term (first term on the left) and the angular diffusion term (first term on the right) are the most important terms in this region of the crack. The second term on the left (angular convection) will become important at larger values of r^*. Attempting a separation of

variables on the two dominant terms leads one to expect a solution of the form

$$c \sim \frac{e^{-K/r^*}}{r^{*s}} f(\theta^*)$$

where K is the separation constant, and f is a function to be determined. The expectation that the angular convection term would become important at larger values of r* suggests that additional terms could be added to this solution in the form

$$c \sim \frac{e^{-K/r^*}}{r^{*s}} f_o(\theta^*) + r^* \frac{e^{-K/r^*}}{r^{*s}} f_1(\theta^*) + r^{*2} \frac{e^{-K/r^*}}{r^{*s}} f_2(\theta^*) + \ldots .$$

This can be recognized as an ordinary perturbation analysis and treatment of equation (7). We are finally lead to adopt the form

$$c = \frac{e^{-K/r^*}}{r^{*1/2}} \sum_{n=o} (r^*)^n f_n(\theta^*) \tag{8}$$

where K is a constant and the f_n's are functions to be determined. Substitution into the equation of convective diffusion gives

$$\begin{gathered} f_o'' + \frac{1}{2}(1-3\theta^{*2}) K f_o = 0 \\ f_o = 0 \text{ at } \theta^* = 1,\ f_o' = 0 \text{ at } \theta^* = 0. \end{gathered} \tag{9}$$

K is an eigenvalue, and f_o is arbitrarily set equal to 1 at $\theta^* = 0$. For $n = 1, 2, 3, ---,$

$$f_n'' + \frac{1}{2}(1-3\theta^{*2})K f_n = \frac{1}{2}\theta^*(1-\theta^{*2})f'_{n-1} - \frac{1}{2}(1-3\theta^{*2})(n-3/2)f_{n-1} = g_n. \tag{10}$$

With this form for c, the neglected radial-diffusion terms become of the same order as the retained terms when r* is of order θ_w.

The solution to the equation (9) is

$$f_o = a_o \left[\left(\frac{3K}{2}\right)^{1/8} e^{-\frac{1}{2}\sqrt{\frac{3K}{2}}\,\theta^{*2}} \; {}_1F_1\left(\frac{\sqrt{\frac{3K}{2}} - \frac{K}{2}}{4\sqrt{\frac{3K}{2}}}, \frac{1}{2}, \sqrt{\frac{3K}{2}}\theta^{*2} \right) \right] \tag{11}$$

where ${}_1F_1(b, d, x)$ is the confluent hypergeometric function. The function has a series form (9)

$${}_1F_1(b, d, x) = 1 + \frac{b}{d}x + \frac{b(b+1)}{2!d(d+1)}x^2 + \cdots\cdots \tag{12}$$

K is chosen such that

$$f_o = 0 \text{ at } \theta^* = 1$$

$$(\text{i.e., } {}_1F_1 = 0 \text{ at } \theta^* = 1). \tag{13}$$

Also, a_o is chosen arbitrarily so that

$$f_o = 1 \text{ at } \theta^* = 0.$$

The solution will be renormalized by "matching" with the outer diffusion layer solution (see below).

For the solution to the nonhomogeneous equation

$$f_n'' + \frac{1}{2}(1-3\theta^{*2})K\, f_n = g_n$$

we try ‡

$$f_n = h_o(\theta^*)\int_o^{\theta^*} g_n f_o(\theta^*)d\theta - f_o(\theta^*)\int_o^{\theta^*} g_n h_o(\theta^*)d\theta + B_n f_o(\theta^*). \tag{14}$$

---

‡Here $h_o = f_o(\theta^*)\displaystyle\int_o^{\theta^*} \frac{d\theta^*}{f_o^{\,2}(\theta^*)}$ is a second solution of the homogeneous equation.

Since f_o is an eigensolution of the homogeneous equation, a solution is possible only if

$$\int_o^1 g_n f_o \, d\theta = 0.$$

This is true for n = 1, and it is this requirement that dictates the power s of r* in the leading term of the solution in equation 8. The value of B_n in the above solution must be selected to meet the requirement

$$\int_o^1 g_{n+1} f_o \, d\theta = 0.$$

Although equation 12 provides an analytic solution to equation 9 for each eigenvalue K, it is not in a convenient form for the calculation of the higher f_n's. From equation 13 it is also difficult to determine the eigenvalues accurately, but it does allow one to estimate the eigenvalues. Therefore, a numerical technique discussed by Newman (10) was used for the calculation of eigenvalues and eigenfunctions. This then allowed the numerical integration of the ordinary, inhomogeneous, linear, second order differential equation (10) for the f_n's. The eigenvalues so obtained were checked by using condition (13).

The equation for f_o, equation 9 is an ordinary, homogeneous, second-order differential equation. It is nonlinear, however, since K is unknown. A second differential equation is introduced

$$\frac{dK}{d\theta^*} = 0, \tag{15}$$

and both f_o and K are unknowns. Equations (9) and (15) are a nonlinear system of two, coupled, ordinary differential equations with boundary conditions

$$f_o = 0 \text{ at } \theta^* = 1$$
$$f_o = 1 \text{ at } \theta^* = 0$$
$$f_o' = 0 \text{ at } \theta^* = 0.$$

The equations can be linearized about a trial solution, producing a series of coupled, linear differential equations. In finite difference form these give coupled, tridiagonal matrices which can be solved on a high-speed, digital computer. The nonlinear problem can then be solved by iteration (see Newman (11)).

The solution for f_n is then determined numerically by evaluating the integrals in equation 14. The linearly independent solution for the homogeneous equation 9 was actually determined by finite difference methods, but with different boundary conditions from those used for f_o.

The mass flux to the walls is determined from the derivatives of the f's at the wall.

The results of these calculations are shown on Figure 2 and Table 1. In Figure 2, only the first three f's are plotted although the first nine were used to calculate the concentration profiles. f_o has a rather simple behavior, beginning at the value of 1 at the crack centerline and decreasing to 0 at the wall. The higher terms have a more complicated behavior. For small values of r*, the first term in the series (equation 8) is dominant and involves only f_o. For larger r*, the higher terms become important and serve to give a concentration profile which shows the greatest change near the wall. This is shown in Figure 3 for two different values of r* At the largest value of r* (r* = 20), the concentration profile is compared to that calculated from the boundary layer results (next section) to demonstrate how well the two agree. More will be said about this later.

In Figure 4 is shown the concentration profile down the crack center line. From these results it is seen that at r* = O(1) the concentration is already very small, and by the time r* becomes of the order of θ_w, where the radial diffusion terms become important in equation 7, c/c_∞ is of the order of 10^{-347}.

These calculations were made for the first eigenvalue, K_o, where

$$K_o = 7.65902.$$

The next higher eigenvalue was found to be

$$K_1 = 150.03633.$$

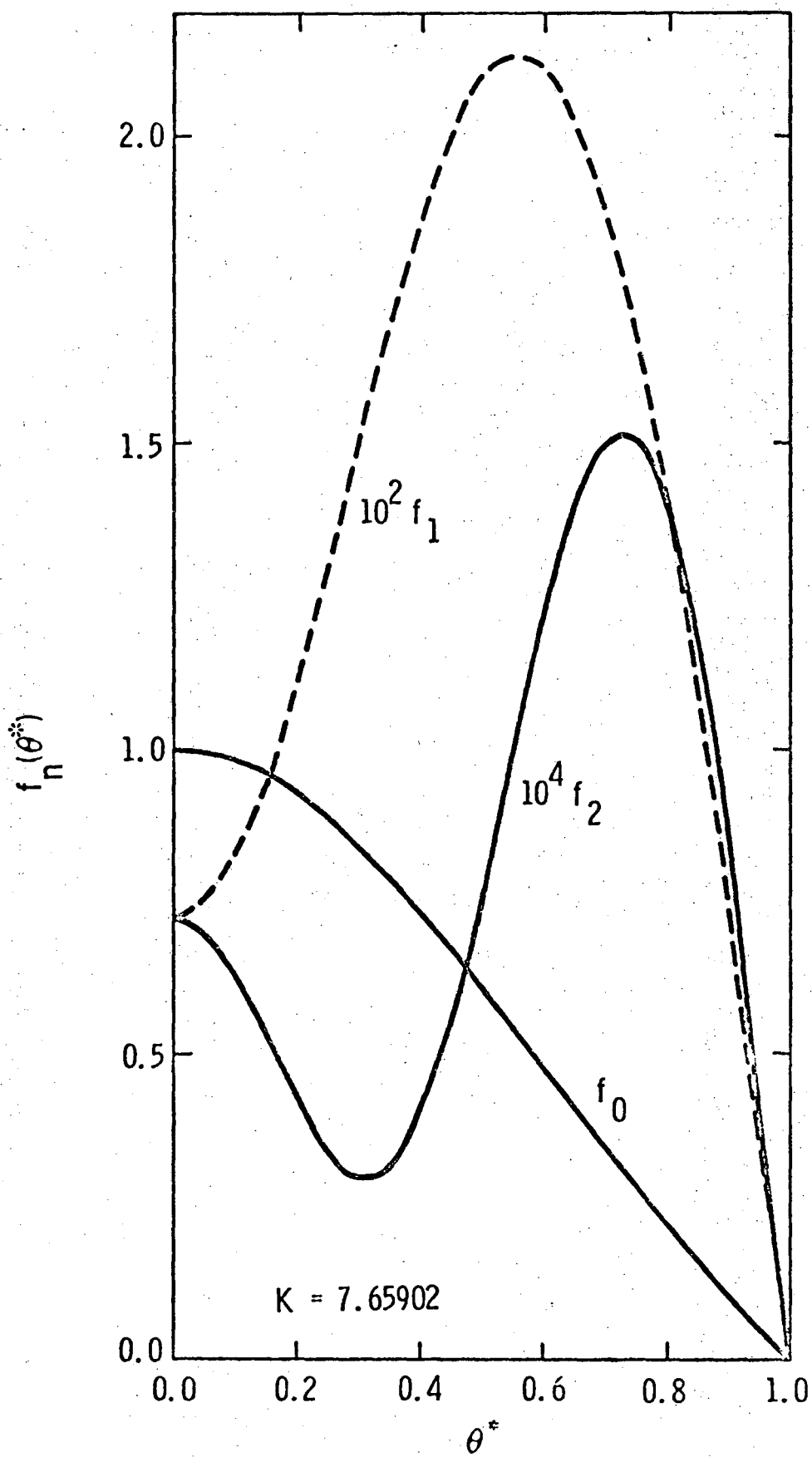

FIGURE 2. $f_n(\theta^*)$ FOR FIRST EIGENVALUE

Table 1

Derivates of the f_n's at the Wall ($\theta^* = 1$)

$$f_o' = -1.0830$$

$$f_1' = -0.07550$$

$$f_2' = -8.866 \times 10^{-4}$$

$$f_3' = +1.744 \times 10^{-5}$$

$$f_4' = -3.297 \times 10^{-7}$$

$$f_5' = +1.335 \times 10^{-8}$$

$$f_6' = -6.893 \times 10^{-10}$$

$$f_7' = +4.501 \times 10^{-11}$$

$$f_8' = -3.455 \times 10^{-12}$$

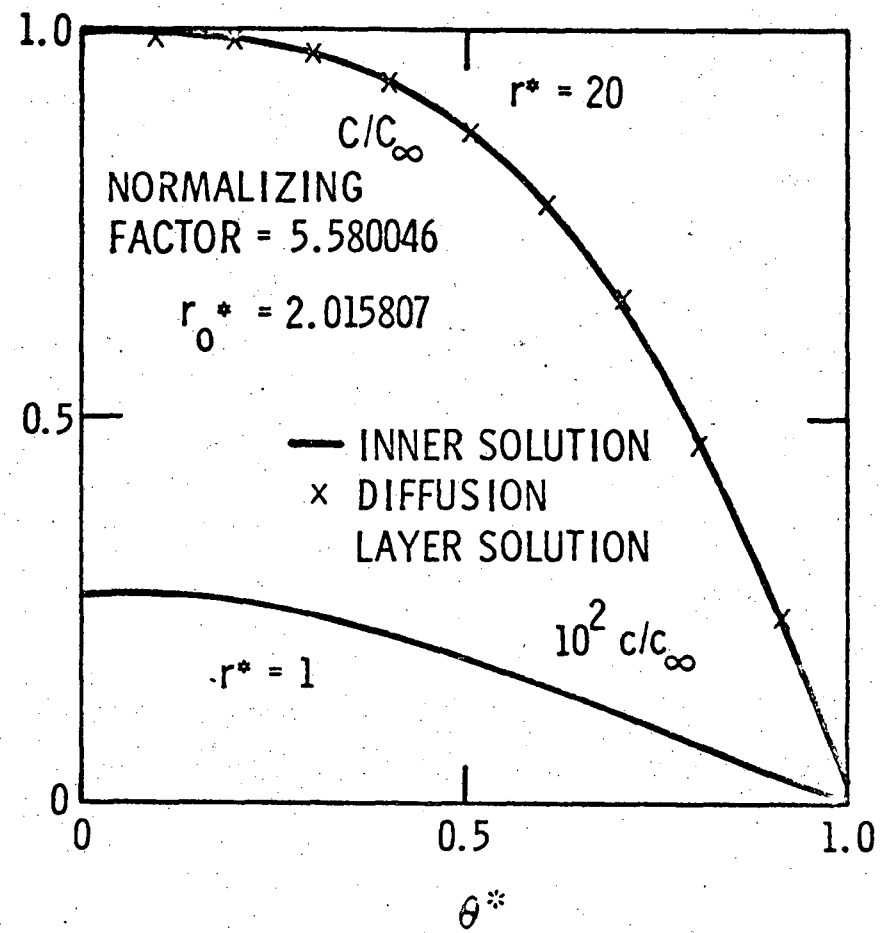

FIGURE 3. CONCENTRATION PROFILES ACROSS CRACK

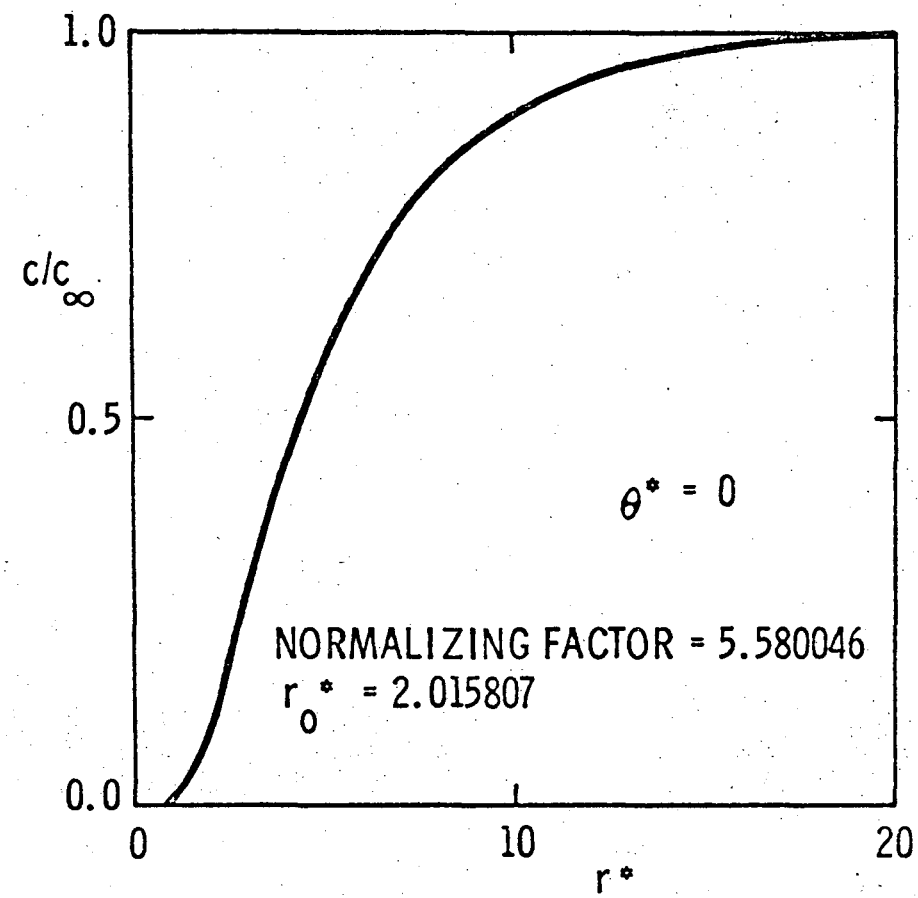

FIGURE 4. CONCENTRATION PROFILE ALONG CRACK CENTER LINE

The complete solution would be expected to be a linear combination of the eigensolutions with the associated eigenvalues. Since the solution for K_1 could not be matched with the boundary layer region, and the concentration profiles across the crack showed an oscillatory behavior, with the concentration even becoming negative, the contribution of this solution to the complete solution must be negligible. Higher eigenvalues and eigensolutions were expected to show similar behavior and therefore were ignored. The lowest solution was judged to be quite adequate for matching all the boundary conditions.

Diffusion layer region

For large values of r^*, the concentration profile showed the greatest variation near the crack wall, and the concentration approached a constant value near the crack center line. The boundary-layer type behavior leads one to search for such a region which would describe the asymptotic characteristics of the region just examined for large values of r^*.

Adopt the variables

$$r^* = r^*$$
$$y = r^*(1-\theta^*).$$

Introducing these variables into (7) and ignoring the radial diffusion terms, we have

$$-\frac{1}{2}\left\{-2 + \frac{6y}{r^*} - 3\left(\frac{y}{r^*}\right)^2\right\}\frac{\partial c}{\partial r^*}$$
$$-\frac{1}{2}\left\{3\left(\frac{y}{r^*}\right)^2 - 2\left(\frac{y}{r^*}\right)^3\right\}\frac{\partial c}{\partial y} = \frac{\partial^2 c}{\partial y^2} \qquad (16)$$

Now, terms of order y/r^* and higher are neglected to yield

$$\frac{\partial c}{\partial r^*} = \frac{\partial^2 c}{\partial y^2} \qquad (17)$$

with boundary conditions

$$c = 0 \text{ at } y = 0$$
$$c = c_\infty \text{ as } y \to \infty.$$

Implicit in these assumptions is the expectation that most of the concentration variation will occur near the wall in this region. Also, the second boundary condition above expresses that the concentration approaches a constant far from the crack wall, and that this constant is the bulk concentration.

Since this is a diffusion-layer region, we try a similarity transformation of 17. The similarity variable is

$$\eta = \frac{y}{g(r^*)}$$

and equation 17 is transformed into two ordinary differential equations

$$\frac{d^2c}{d\eta^2} + 2\eta \frac{dc}{d\eta} = 0 \qquad (18)$$

$$g\frac{dg}{dr^*} = 2 \qquad (19).$$

The solutions to these equations are

$$c = \frac{2c_\infty}{\sqrt{\pi}} \int_0^\eta e^{-x^2}\, dx = c_\infty \operatorname{erf}(\eta) \qquad (20)$$

$$g = (4r^* + 4r_o^*)^{1/2} \qquad (21).$$

Equation 20 is the error function solution which is commonly encountered in diffusion-layer problems and is tabulated by Abramowitz and Stegun (12). The constant r_o^* in (21) may be arbitrarily chosen to give the best "match" with the solution from the region where $r^* = O(1)$ (see for example Van Dyke (13)).

The concentration profile given by (20) has been shown already in Figure 3. The comparison there indicates that the diffusion-layer solution provides a good description of the asymptotic behavior of (8) for values of r^* of about 20 and above.

In Figure 5 the flux to the wall is plotted as a function of r^*. The solid line was calculated from the solution obtained in the $r^* = O(1)$ region. The dotted line was calculated from the diffusion-layer results. There is a good match for values of r^* greater than about 10. This could be viewed as the inner limit of validity of the diffusion layer results. One also notes that for $r^* = O(1)$, the flux has decreased markedly to near zero. For $r^* = O(\theta_w)$, the flux is so small as to be insignificant.

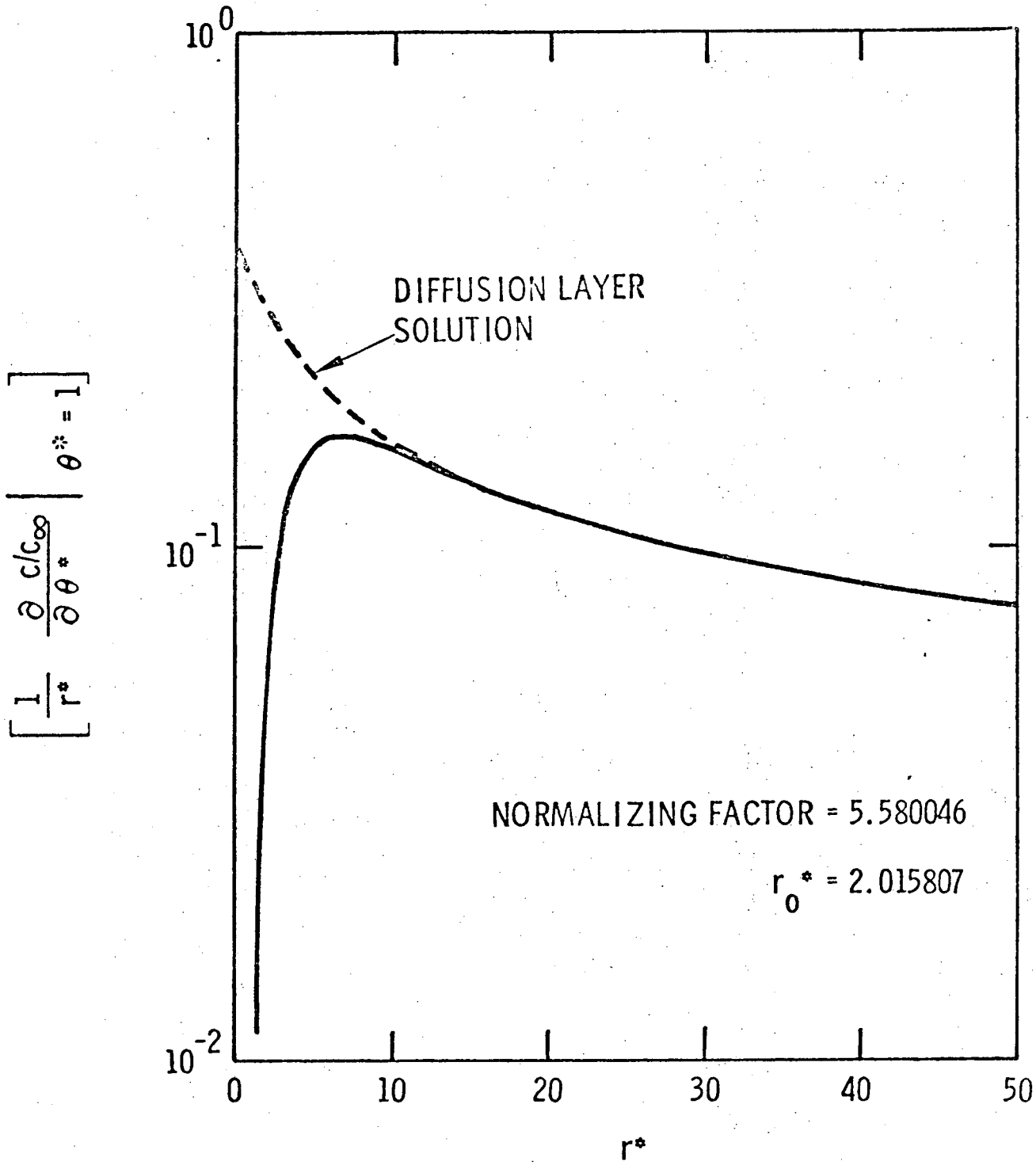

FIGURE 5. FLUX TO THE WALL

Matching of results

Figure 3 and 5 indicate that the results from the two regions agree and may be "matched". The procedure for doing this was as follows. It was noted that the concentration along the crack center line approached an asymptotic value as r^* approached 20 (see Figure 4). This value is the bulk concentration, c_∞. Using $c/c_\infty \to 1$ as $r^* \to 20(\theta^* = 0)$, one may renormalize equation 8 (essentially renormalize f_o at $\theta^* = 0$). This normalization factor was 5.580046. This value of the constant was then used to calculate the concentration profile across the crack. The agreement between the inner region and the diffusion layer region was good at large r^*. It was found that the match could be improved, however, by choosing a value of r_o^* (see equation 21) of

$$r_o^* = 2.015807.$$

The results have been given in Figures 3 and 5. The justification for choosing this constant to give the best match has been discussed by Van Dyke (13). Thus, equation 8 gives an adequate description of the results for $\theta_w < r^* \leq 20$. The diffusion-layer solution should be used for larger values of r^*.

Other regions

Far from the crack tip, outside the diffusion layer, the concentration is constant and is identical to the bulk concentration. That is, there is no effect of diffusion in this region and no other mechanism to create concentration differences.

For values of r^* of the order of θ_w, all terms in equation 7 are important. The concentration and flux to the wall have already decreased to such a low level that one can ignore them for the purposes of this paper. For $r^* = O(\theta_w)$,

$$r = O\left(\frac{D}{\theta_w V}\right) = O(10^{-3}\ \text{cm}).$$

At still smaller values of r^*, i.e., $r^* = O(\theta_w^2)$ or $r \approx 10^{-5}$ cm, only the diffusion terms are important in equation 7. Here again, the exceedingly small values of concentration and flux make this region unimportant for the present treatment.

Summary

As a summary, Figure 6 indicates the different regions that have been revealed in this investigation and the different modes of mass transfer in them. Again, for distances nearer the crack tip than 10^{-3} cm, the solution is essentially devoid of the reactive species.

Conclusions

From the results of this study, it may be concluded that minor components being consumed in a crack at rates limited by mass transfer have vanishingly small concentrations near the crack tip. It is unlikely that such species would be important as critical species in crack extension processes. More specifically, small amounts of OH^-, H_2O, or O_2 dissolved in molten LiCl-KCl can not be critical species in the cracking of Ti 8-1-1.

It is tempting to extrapolate the results to solutions of higher concentration. One would be led to conclude that none of the reactive species could get to the crack tip, no matter what the bulk concentration. However, this conclusion is probably not justified, because it is doubtful if the same analysis could be used for more concentrated solutions. One could expect in such solutions that the mass transfer processes could change the fluid-flow characteristics, with results which might be quite different than those found here.

Other extensions of the present treatment intended for future considerations are:

(1) the inclusion of more complicated boundary conditions such as the hindered electrochemical kinetics of the wall reactions;

(2) inclusion of the effects of dissolution at the wall;

(3) treatment of dissolution at the crack tip, with cathodic reactions on the wall, and;

(4) extension to geometries with "rounded" crack tips.

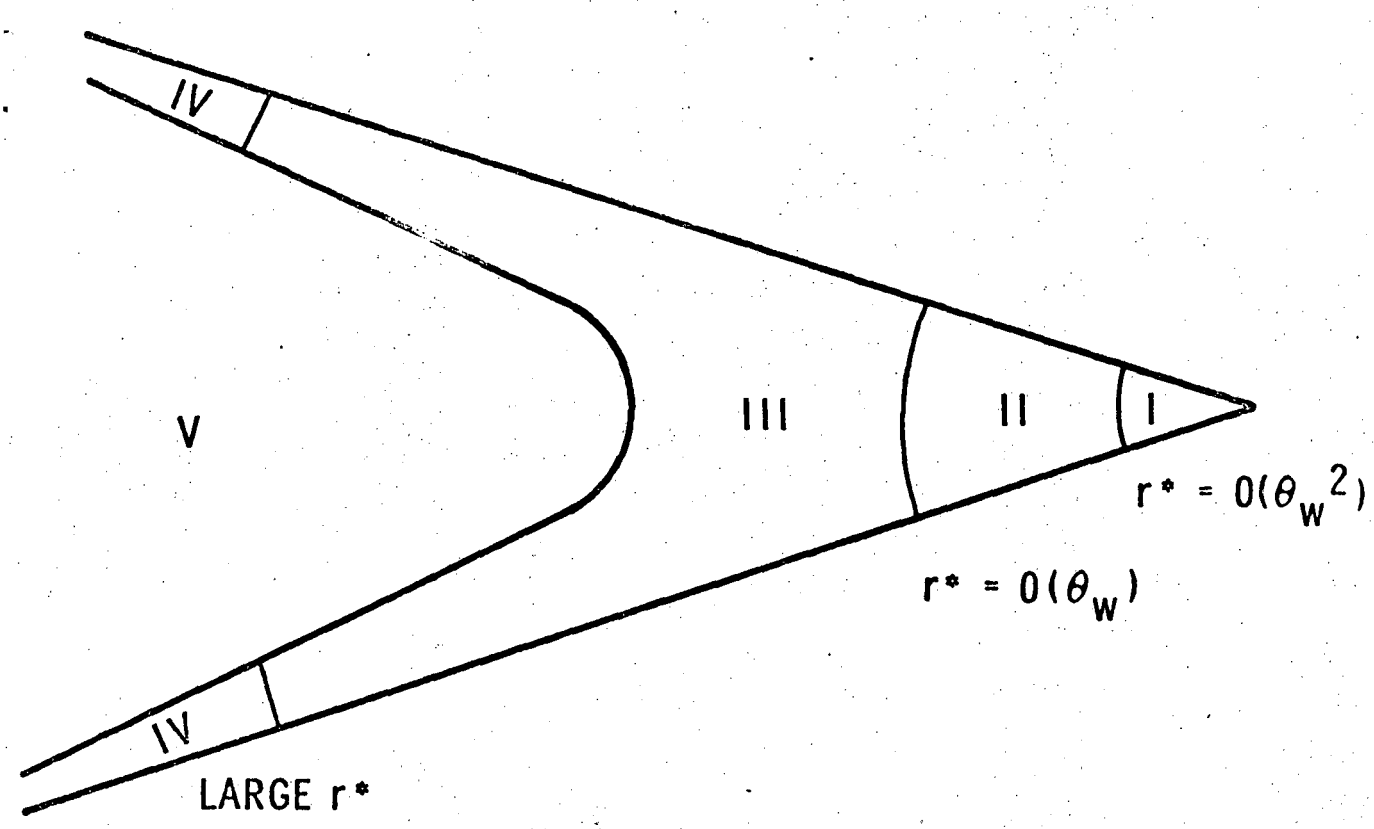

REGION:
- I DIFFUSION ONLY
- II ALL TERMS IMPORTANT
- III RADIAL DIFFUSION NEGLIGIBLE
- IV RADIAL CONVECTION, ANGULAR DIFFUSION
- V CONCENTRATION CONSTANT

FIGURE 6. REGIONS OF MASS TRANSFER

Nomenclature

c	concentration (moles/cm^3)
D	diffusion coefficient (cm^2/sec)
$f_n(\theta^*)$	functions defined in equation (8)
${}_1F_1$	confluent hypergeometric function
$g_n(\theta^*)$	functions defined in equation (10)
h_o	function defined in footnote, page 7
K	constant defined in equation (8)
r	radial dimension (cm)
r^*	dimensionless variable
v_r	radial component of liquid velocity in crack (cm/sec)
v_θ	angular component of liquid velocity in crack (cm/sec)
V	velocity of crack propagation (cm/sec)
y	dimensionless variable
θ	angular dimension
θ_w	crack angle
θ^*	reduced variable
η	similarity variable
ν	fluid kinematic viscosity (cm^2/sec)

List of Figure Titles

Figure 1 Fluid Flow in a Propagating Crack

Figure 2 $f_n(\theta^*)$ for First Eigenvalue

Figure 3 Concentration Profiles Across Crack

Figure 4 Concentration Profile Along Crack Center Line

Figure 5 Flux to the Wall

Figure 6 Regions of Mass Transfer

REFERENCES

1. M. J. Blackburn, J. A. Feeney, and T. R. Beck, "Stress Corrosion Cracking of Titanium Alloys," Advances in Corrosion Science and Corrosion Engineering, Vol. 3, M. G. Fontana and R. W. Staehle, Eds. Plenum Press, New York, 1973.

2. Markus O. Speidel and Michael V. Hyatt, "Stress-Corrosion Cracking of High Strength Aluminum Alloys," Vol. 2, Advances in Corrosion Science and Corrosion Engineering, M. G. Fontana and R. W. Staehle, Eds., Plenum Press, New York, 1972.

3. M. J. Blackburn, W. H. Smyrl, and J. A. Feeney, "Engineering Aspects of the Stress Corrosion Cracking of Titanium Alloys," in State of the Art: Stress Corrosion Cracking, B. F. Brown, Editor.

4. S. M. Wiederhorn, "Influence of Water Vapor on Crack Propagation in Soda-Lime Glass," J. Amer.Cer.Soc. 50, 407-14, 1967.

5. T. R. Beck and E. A. Grens, "An Electrochemical Mass-Transport-Kinetic Model for Stress-Corrosion Cracking of Titanium," J.Electrochem.Soc.116, 177 (1969).

6. T. R. Beck, "Electrochemical Models for SCC of Titanium," in The Theory of Stress Corrosion Cracking in Alloys, J. C. Scully, Ed., Brussels, NATO, 1971.

7. W. H. Smyrl and M. J. Blackburn, "Stress Corrosion Cracking in Molten Salts," Proceedings of the International Symposium on Stress Corrosion Mechanisms in Titanium Alloys, Atlanta, Georgia, January 1971 (to be published).

8. John Newman and W. H. Smyrl, "Fluid Flow in a Propagating Crack," Met.Trans. (accepted for publication).

9. P. M. Morse and H. Feshbach, Methods of Theoretical Physics, Part I, McGraw-Hill, Inc., New York, 1953, p. 604.

10. John Newman, "The Fundamental Principles of Current Distribution and Mass Transport in Electrochemical Cells," Electronanalytical Chemistry, Vol. 6, pp. 187-352, A. J. Bard, Ed, Marcel Dekker, Inc. New York 1973.

11. John Newman, "Numerical Solution of Coupled, Ordinary Differential Equations," Ind. Engr. Chem. Fund. 7, 514 (1968)

12. M. Abramowitz and I. A. Stegun, Handbook of Mathematical Functions, Dover Publications, Inc., New York, 1965.

13. M. VanDyke, Perturbation Methods in Fluid Mechanics, Academic Press, New York, 1964.

LEGAL NOTICE

This report was prepared as an account of work sponsored by the United States Government. Neither the United States nor the United States Atomic Energy Commission, nor any of their employees, nor any of their contractors, subcontractors, or their employees, makes any warranty, express or implied, or assumes any legal liability or responsibility for the accuracy, completeness or usefulness of any information, apparatus, product or process disclosed, or represents that its use would not infringe privately owned rights.

TECHNICAL INFORMATION DIVISION
LAWRENCE BERKELEY LABORATORY
UNIVERSITY OF CALIFORNIA
BERKELEY, CALIFORNIA 94720